Towards reliable and efficient modeling of $[Cu_2O_2]^{2+}$-based compound electronic structures with the partially fixed reference space protocols†

Matheus Morato F. de Moraes[‡a], and Paweł Tecmer[*a]

Electronic Supporting Information

[a] *Institute of Physics, Faculty of Physics, Astronomy, and Informatics, Nicolaus Copernicus University in Toruń, Grudziadzka 5, 87-100 Toruń, Poland;*
[‡] *matheusmorat@gmail.com;* [*] *ptecmer@fizyka.umk.pl*

S1 Isolated copper orbital optimization

The seminal articles by Hay[1] showed that the optimal radial function of the $3d$ orbital (measured by the expected value of the radial operator) largely depends on the number of $3d$ electrons in the configuration. On the other hand, for a specific $3d$ occupation, the environmental effect over the $3d$ optimal set (the change in charge can emulate that) is one order of magnitude smaller[2] as exemplified in Table S1 for the copper atom and its cations. Additionally, spatial and spin symmetry has almost no effect over the radial function of the optimal $3d$ orbital.[2] For example, the change in $\langle \hat{r}_d \rangle$ among $Cu^{2+}(3d^8 4s^1;^4F_g)$, $Cu^{2+}(3d^8 4s^1;^2F_g)$ and $Cu^{2+}(3d^8 4s^1;^2D_g)$ is in the order of 0.001 a_0. Lastly, the increase of the basis set (from DZ up to 5Z) has no effect over the optimal $3d$ orbital.

To optimize the atomic $3d$-shell for each $3d$-occupancy we followed the procedure described in Ref.[3] A weighted state average CASSCF calculation between two sets of states with distinct $3d$ occupations. That is,

$$\min_{\boldsymbol{c},\boldsymbol{C}} \left(\frac{1-m}{n_p} \sum_{i=1}^{n_p} \frac{\langle \Psi_i(3d^p)|\hat{H}|\Psi_i(3d^p)\rangle}{\langle \Psi_i(3d^p)|\Psi_i(3d^p)\rangle} + \frac{m}{n_{p+1}} \sum_{j=1}^{n_{p+1}} \frac{\langle \Psi_j(3d^{p+1})|\hat{H}|\Psi_j(3d^{p+1})\rangle}{\langle \Psi_j(3d^{p+1})|\Psi_j(3d^{p+1})\rangle} \right), \tag{1}$$

where $\boldsymbol{c}$ and $\boldsymbol{C}$ are the orbitals and CI coefficients, respectively. p is the number of $3d$ electrons in each configuration, n_p is the number of states ($\Psi_i(3d^p)$) with $3d^p$ configurations considered, and m is the relative weight between the $3d^p$ and $3d^{p+1}$ states in the weighted-state-average framework. As neither the state symmetries nor the system charge profoundly affects the optimized $3d$ orbitals, the choice of states was based on how challenging the convergence is. Therefore, the $Cu^+(3d^8 4s^2;^3F_g)$, $Cu^+(3d^9 4s^1;^3D_g)$, and $Cu^0(3d^{10} 4s^1;^2S_g)$ for optimal $3d^8$, $3d^9$ and $3d^{10}$, respectively. For the intermediate set of orbitals, with a radial function between two optimal ones, we used a value of m equal to 0.6. Such a choice was based on the results of previous works.[2–4] A minimal input file for MOLPRO can be found in the supporting information of reference[3].

Table S1 Expected value of the $\hat{r}$ operator (in a_0) for the $3d$ orbital, $\langle \hat{r}_d \rangle$, for a set of charges and configurations of the isolated copper atom.

	Optimized configuration		
charge (c)	$3d^8 4s^{3-c}$	$3d^9 4s^{2-c}$	$3d^{10} 4s^{1-c}$
-1	—	—	1.002
0	—	0.924	0.997
1	0.862	0.916	0.984
2	0.856	0.905	—
3	0.848	—	—

S2 In-depth analysis of the PFRS-V2 results

Analyzing the ground state CAS(4,4), PFRS-V2 wave function at the D_{2h}, we observe that one b_{3u} is mainly doubly occupied throughout the geometries and one b_{2g} primarily unoccupied. We obtain a two-active orbital set and a two-configuration reference space by closing the former and removing the latter. The active orbitals consist of an almost pure b_{3u} $3d^-_{xz}$ orbital, that is, the subtraction between the $3d_{xz}$ of each copper, and a b_{2g} that mixes the copper $3d^+_{xz}$ and oxygen $2p^-_z$ orbitals (the localized copper orbitals and symmetric adapted oxygen ones are qualitatively the same as the ones shown in Figure 3 of the main text). At f=0, the b_{2g} is mainly $3d^+_{xz}$ with a small contribution of the $2p^-_z$ and the wave function is 60% $|b^2_{3u}\rangle$ and 40% $|b^2_{2g}\rangle$. Approximately, this function can be expressed as,

$$|\Psi(1O)\rangle \approx 0.8 \left| \left(\frac{3d_L - 3d_R}{\sqrt{2}} \right)^2 \right\rangle - 0.6 \left| \left(\frac{3d_L + 3d_R}{\sqrt{2}} \right)^2 \right\rangle, \tag{2}$$

with $3d_L$ and $3d_R$ representing the localized $3d_{xz}$-orbitals from the left and right copper centers, respectively. Expanding this approximated wave function as follows, it is possible to have a rough estimation of the $3d$-occupation,

$$\begin{aligned}
|\Psi(1O)\rangle \approx & \frac{0.8}{2}[|3d^2_L\rangle + |3d^2_R\rangle - (|3d_L 3\bar{d}_R\rangle + |3d_R 3\bar{d}_L\rangle)] \\
& - \frac{0.6}{2}\left[|3d^2_L\rangle + |3d^2_R\rangle + \left(|3d_L 3\bar{d}_R\rangle + |3d_R 3\bar{d}_L\rangle \right) \right] \\
= & 0.1\left(|3d^2_L\rangle + |3d^2_R\rangle) \right) - \frac{1.4}{2}\left(|3d_L 3\bar{d}_R\rangle + |3d_R 3\bar{d}_L\rangle \right) \\
\approx & \frac{1}{\sqrt{2}}\left(|3d_L 3\bar{d}_R\rangle + |3d_R 3\bar{d}_L\rangle \right),
\end{aligned} \tag{3}$$

where bar orbitals indicate singly occupied down electrons. The CAS(2,2) results in an almost pure $d^{9\text{-}9}$-occupancy wave function with a singlet bi-radical character at f=0. Therefore, as discussed in detail by Gherman and Cramer,[5] a smaller active space (i.e., a single Slater determinant) would be unable to represent the bi-radical character and, consequently, result in a forced $d^{10\text{-}10}$-occupancy. The increase of the d^9-occupancy over the d^{10} one may once again be attributed to the lack of oxygen $2p$ orbitals excitation seen in the $d^{9\text{-}10}$ and $d^{10\text{-}10}$ configurations. On the other hand, at f=1, the b_{2g} active orbital became an almost equal copper/oxygen mixing, $(3d^{+}_{xz}+2p^{-}_{z})/\sqrt{2}$, with its counterpart orbital, $(3d^{+}_{xz}-2p^{-}_{z})/\sqrt{2}$, in the closed space. At this geometry, the wave function is less multirreferential with 85% $|b^2_{3u}\rangle$ and 15% $|b^2_{2g}\rangle$. In this case, expanding the approximated wave functions is slightly more laborious as the $3d_{xz}+2p_z$ orbital must be considered, but results in

$$
\begin{aligned}
|\Psi(1P)\rangle \approx & 0.91\left|\left(\frac{3d_L+3d_R}{2}-\frac{p^{-}_{z}}{\sqrt{2}}\right)^2\left(\frac{3d_L-3d_R}{\sqrt{2}}\right)^2\right\rangle \\
& -0.39\left|\left(\frac{3d_L+3d_R}{2}-\frac{p^{-}_{z}}{\sqrt{2}}\right)^2\left(\frac{3d_L+3d_R}{2}+\frac{p^{-}_{z}}{\sqrt{2}}\right)^2\right\rangle \\
\approx & 0.13(|(p^{-}_{z})^2 3d^2_L\rangle+|(p^{-}_{z})^2 3d^2_R\rangle) \\
& -0.60\left(\frac{|(p^{-}_{z})^2 3d_L 3\bar{d}_R\rangle+|(p^{-}_{z})^2 3d_R 3\bar{d}_L\rangle}{\sqrt{2}}\right) \\
& -0.455\left(\frac{|3d^2_R 3d_L \bar{p}^{-}_{z}\rangle+|3d^2_R p^{-}_{z} 3\bar{d}_L\rangle}{\sqrt{2}}\right. \\
& \left.-\frac{|3d^2_L 3d_R \bar{p}^{-}_{z}\rangle+|3d^2_L p^{-}_{z} 3\bar{d}_R\rangle}{\sqrt{2}}-|3d^2_L 3d^2_R\rangle\right).
\end{aligned}
\tag{4}
$$

In this case, the wave function still has a large $d^{9\text{-}9}$ component (around 36%), but the $d^{9\text{-}10}$ component is now the main configuration of the wave function (41%), with a somehow smaller importance of $d^{10\text{-}10}$ (20%). The wave function and orbitals coefficients are listed in Table S8. That way, the minimum small active space does have a more considerable bias toward the d^9-occupancy if compared with our previous CAS(4,4) and RAS(28,18) calculations.

S3 MRCCSD dependence on the SVD threshold

Figure 9.a of the main text PEC shape slightly depends on the threshold value for geometries close to the 2P (around f=0.8). That dependence increases significantly towards the 2O structure. For example, using a 10^{-4} threshold value the CAS(4,4)PFRS-V2/MRCCSD the relative energy values follows the CAS(12,10)PFRS-V2/NEVPT2 closely from f=0 to f=0.8 (Figure 9.b). The relative energy between minima goes from around 8 kcal/mol using a 10^{-4} threshold value to 3 kcal/mol using a 10^{-6}. For the barrier (around f=0.3), the use of a 10^{-6} threshold value does not result in a continuous PEC, while no convergence is reached using values 10^{-7} or lower. The automatic definition of the SVD for the icMRCCSD method is an open problem, and its use is known to cause discontinues.[6,7] On the other hand, testing the convergence with the SVD threshold value is computationally costly and time-consuming, particularly in cases where the side that leads to accurate values is close to the ones that lead to non-convergence. Moreover, correlation difficulties with the SVD threshold are not correlated with the quality of the orbitals or reference wave function but depend on the excitation operation choice and virtual orbital space basis.[7] Therefore, with an extensive SVD values scan, it should be possible to have a better-behaved PEC.

	1O/1P		
Atom	x	y	z
Cu	0.00	0.00	ZCu(f)
Cu	0.00	0.00	-ZCu(f)
O	XO(f)	0.00	0.00
O	-XO(f)	0.00	0.00

	2O/2P			3O/3P			4O/4P		
Atom	x	y	z	x	y	z	x	y	z
Cu	0.00	0.000	ZCu(f)	0.00	0.000	ZCu(f)	0.00	0.000	ZCu(f)
Cu	0.00	0.000	-ZCu(f)	0.00	0.000	-ZCu(f)	0.00	0.000	-ZCu(f)
O	XO(f)	0.000	0.00	XO(f)	0.000	0.00	XO(f)	0.000	0.00
O	-XO(f)	0.000	0.00	-XO(f)	0.000	0.00	-XO(f)	0.000	0.00
N	1.41	0.000	ZN(f)	1.41	0.000	ZN(f)	0.000	1.41	ZN(f)
N	-1.41	0.000	ZN(f)	-1.41	0.000	ZN(f)	0.000	-1.41	ZN(f)
N	1.41	0.000	-ZN(f)	0.000	1.41	-ZN(f)	0.000	1.41	-ZN(f)
N	-1.41	0.000	-ZN(f)	0.000	-1.41	-ZN(f)	0.000	-1.41	-ZN(f)
H	2.32	0.000	ZH2(f)	2.32	0.000	ZH2(f)	0.000	2.32	ZH2(f)
H	-2.32	0.000	ZH2(f)	-2.32	0.000	ZH2(f)	0.000	-2.32	ZH2(f)
H	2.32	0.000	-ZH2(f)	0.000	2.32	-ZH2(f)	0.000	2.32	-ZH2(f)
H	-2.32	0.000	-ZH2(f)	0.000	-2.32	-ZH2(f)	0.000	-2.32	-ZH2(f)
H	1.32	0.814	ZH(f)	1.32	0.814	ZH(f)	0.814	1.32	ZH(f)
H	-1.32	-0.814	ZH(f)	-1.32	-0.814	ZH(f)	-0.814	-1.32	ZH(f)
H	-1.32	0.814	-ZH(f)	0.814	-1.32	-ZH(f)	0.814	-1.32	-ZH(f)
H	1.32	-0.814	-ZH(f)	-0.814	1.32	-ZH(f)	-0.814	1.32	-ZH(f)
H	1.32	-0.814	ZH(f)	1.32	-0.814	ZH(f)	-0.814	1.32	ZH(f)
H	-1.32	0.814	ZH(f)	-1.32	0.814	ZH(f)	0.814	-1.32	ZH(f)
H	-1.32	-0.814	-ZH(f)	-0.814	-1.32	-ZH(f)	-0.814	-1.32	-ZH(f)
H	1.32	0.814	-ZH(f)	0.814	1.32	-ZH(f)	0.814	1.32	-ZH(f)

ZN(f)=0.40f+2.81 ZH(f)=0.40f+3.39 ZH2(f)=0.40f+2.39
ZCu(f)=0.40f+1.40 XO(f)=-0.45f+1.15

Table S2 Cartesian coordinates of the model systems, depicted in Figure 1, based on Cramer *et al.* structures.[8]

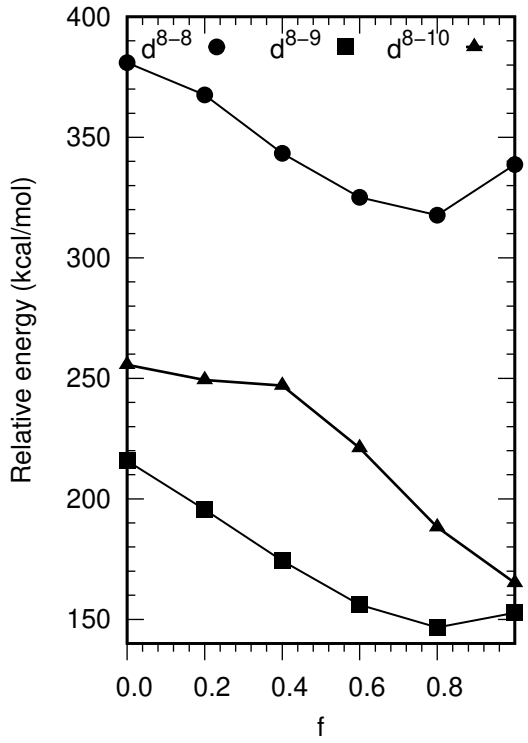

Fig. S1 States with d^8-occupancies for the $[Cu_2O_2]^{2+}$ model system.

	1^1A_1		
f	$d^{9\text{-}9}$	$d^{9\text{-}10}$	$d^{10\text{-}10}$
0.0	-3455.227564890512	-3455.136611135186	-3455.098292181340
0.2	-3455.252144397374	-3455.156383094381	-3455.116643704130
0.4	-3455.272871647784	-3455.196393099830	-3455.141616697286
0.6	-3455.287803257683	-3455.241717684979	-3455.176234417951
0.8	-3455.284248415589	-3455.276779293970	-3455.223426685217
1.0	-3455.261842356613	-3455.296883994220	-3455.273065750998

	2^1A_1		
f	$d^{9\text{-}9}$	$d^{9\text{-}10}$	$d^{10\text{-}10}$
0.0	-3455.227408862293	-3455.120336018009	-3455.072901963569
0.2	-3455.251729272204	-3455.154240929347	-3455.080328038855
0.4	-3455.272601284350	-3455.172366422580	-3455.086909776513
0.6	-3455.287637762246	-3455.197447980219	-3455.113779920945
0.8	-3455.283839230926	-3455.233061925377	-3455.159973230064
1.0	-3455.261841700184	-3455.256483360133	-3455.206982131291

	3^1A_1		
f	$d^{9\text{-}9}$	$d^{9\text{-}10}$	$d^{10\text{-}10}$
0.0	-3455.226593247568	-3455.099324723309	-3455.044911628105
0.2	-3455.251296496599	-3455.120973158460	-3455.053434951854
0.4	-3455.271631927691	-3455.156320506687	-3455.078181770053
0.6	-3455.285758423840	-3455.179591880349	-3455.088152965162
0.8	-3455.280968394783	-3455.159918257141	-3455.076844883040
1.0	-3455.258074832266	-3455.197721684115	-3455.015359492959

	4^1A_1		
f	$d^{9\text{-}9}$	$d^{9\text{-}10}$	$d^{10\text{-}10}$
0.0	-3455.222519433927	-3455.098709578811	-3455.036464674067
0.2	-3455.247701203325	-3455.117657853217	-3455.039059096082
0.4	-3455.269722650679	-3455.144675179939	-3455.025009764029
0.6	-3455.285163840013	-3455.163272139090	-3454.989818211693
0.8	-3455.280863859661	-3455.134811228217	-3454.949067368989
1.0	-3455.258051000370	-3455.188303056069	-3454.875133505563

	5^1A_1		
f	$d^{9\text{-}9}$	$d^{9\text{-}10}$	$d^{10\text{-}10}$
0.0	-3455.221965156033	-3455.096695604350	-3454.931066830939
0.2	-3455.247618824352	-3455.115975509038	-3454.944351203716
0.4	-3455.269612218011	-3455.131584380099	-3454.959414637541
0.6	-3455.285036823410	-3455.137281179306	-3454.966613693231
0.8	-3455.279929338988	-3455.108100689388	-3454.914722093281
1.0	-3455.256687880774	-3455.179808780421	-3454.817958469786

Table S3 Total energy (in E_h) of the five low-lying d-occupancy-specific states shown in Figure 4.

	1^1A_1				6^1A_1			
f	Total Energy	$d^{9\text{-}9}$	$d^{9\text{-}10}$	$d^{10\text{-}10}$	Total Energy	$d^{9\text{-}9}$	$d^{9\text{-}10}$	$d^{10\text{-}10}$
0.0	-3455.253569468233	43.9	44.5	11.6	-3455.186108285989	61.2	33.9	4.9
0.2	-3455.268635934172	42.0	43.7	14.3	-3455.187761584177	57.1	36.7	6.2
0.4	-3455.285423446654	40.9	44.0	15.0	-3455.192865011932	69.3	25.8	4.9
0.6	-3455.298293367625	37.4	45.6	16.9	-3455.189279324857	87.1	12.4	0.5
0.8	-3455.307142505761	25.3	51.6	23.1	-3455.176184860682	86.7	12.9	0.4
1.0	-3455.320935488856	7.0	50.2	42.7	-3455.178822051609	4.9	95.0	0.0

	2^1A_1				7^1A_1			
f	Total Energy	$d^{9\text{-}9}$	$d^{9\text{-}10}$	$d^{10\text{-}10}$	Total Energy	$d^{9\text{-}9}$	$d^{9\text{-}10}$	$d^{10\text{-}10}$
0.0	-3455.246698477975	41.1	44.8	14.1	-3455.181468211818	60.2	35.3	4.5
0.2	-3455.243406122214	41.0	45.8	13.2	-3455.178350807006	64.8	30.0	5.2
0.4	-3455.226720642387	38.3	46.6	15.1	-3455.177949560290	82.7	15.9	1.3
0.6	-3455.218856767372	36.4	47.6	16.0	-3455.189217599823	87.0	12.4	0.6
0.8	-3455.229536301751	14.5	64.8	20.7	-3455.175841419220	87.5	12.4	0.2
1.0	-3455.267791732838	1.7	42.0	56.3	-3455.169860599631	77.4	21.8	0.8

	3^1A_1				8^1A_1			
f	Total Energy	$d^{9\text{-}9}$	$d^{9\text{-}10}$	$d^{10\text{-}10}$	Total Energy	$d^{9\text{-}9}$	$d^{9\text{-}10}$	$d^{10\text{-}10}$
0.0	-3455.211158270339	46.6	40.6	12.9	-3455.178603211014	62.8	34.1	3.1
0.2	-3455.218907433178	45.5	41.7	12.8	-3455.176312313220	63.1	32.1	4.8
0.4	-3455.216856344304	40.7	44.4	14.9	-3455.176862620391	84.8	14.5	0.7
0.6	-3455.206428304294	78.8	19.5	1.7	-3455.172149120971	95.3	4.5	0.2
0.8	-3455.195091057447	78.9	19.6	1.5	-3455.156080323352	96.4	3.5	0.1
1.0	-3455.222436854566	2.7	96.7	0.6	-3455.167466742264	82.6	17.3	0.1

	4^1A_1				9^1A_1			
f	Total Energy	$d^{9\text{-}9}$	$d^{9\text{-}10}$	$d^{10\text{-}10}$	Total Energy	$d^{9\text{-}9}$	$d^{9\text{-}10}$	$d^{10\text{-}10}$
0.0	-3455.205304009300	49.0	38.9	12.1	-3455.172340671517	66.5	30.6	2.9
0.2	-3455.208991339536	50.0	39.2	10.8	-3455.170631187243	64.8	32.3	2.9
0.4	-3455.198834815581	59.2	36.1	4.7	-3455.175643852918	53.1	38.4	8.6
0.6	-3455.201905201529	66.0	31.6	2.5	-3455.167677257960	72.6	22.7	4.7
0.8	-3455.192855181709	29.0	66.9	4.1	-3455.151975930448	59.0	16.3	24.6
1.0	-3455.198078080698	3.6	59.0	37.4	-3455.157386452726	87.9	12.1	0.0

	5^1A_1				10^1A_1			
f	Total Energy	$d^{9\text{-}9}$	$d^{9\text{-}10}$	$d^{10\text{-}10}$	Total Energy	$d^{9\text{-}9}$	$d^{9\text{-}10}$	$d^{10\text{-}10}$
0.0	-3455.191898743259	58.5	35.9	5.7	-3455.172036277156	66.7	31.7	1.6
0.2	-3455.196020083061	55.4	37.5	7.0	-3455.166502419549	69.4	29.8	0.8
0.4	-3455.194166139296	52.4	36.4	11.2	-3455.172072568204	71.0	27.2	1.7
0.6	-3455.201190195637	31.3	51.6	17.1	-3455.159424747311	66.3	27.1	6.5
0.8	-3455.190475988893	40.1	57.6	2.3	-3455.149117467263	27.4	65.3	7.4
1.0	-3455.184270879678	69.8	29.9	0.3	-3455.153191076080	93.4	6.5	0.1

Table S4 Numerical values from Figure 5 of the main text. Total energies in atomic unities (E_h) and the d columns represent the sum of squared coefficient (in percentage) for each pair of d-occupancies in each root wave function

	1^1A_1											
	cc-pVTZ-DK				cc-pVQZ-DK				cc-pV5Z-DK			
f	Energy	$d^{9\text{-}9}$	$d^{9\text{-}10}$	$d^{10\text{-}10}$	Energy	$d^{9\text{-}9}$	$d^{9\text{-}10}$	$d^{10\text{-}10}$	Energy	$d^{9\text{-}9}$	$d^{9\text{-}10}$	$d^{10\text{-}10}$
0.0	-0.31451537	50.5	41.1	8.3	-0.34995751	53.9	39.3	6.8	-0.36563432	56.1	38.0	5.8
0.2	-0.32492757	47.8	40.4	11.8	-0.35754143	51.4	38.8	9.9	-0.37281037	53.7	37.4	8.9
0.4	-0.33915820	46.6	41.7	11.7	-0.36903704	50.5	39.5	10.0	-0.38386415	53.5	37.5	9.0
0.6	-0.34946475	43.5	43.1	13.4	-0.37730382	47.7	40.8	11.6	-0.39103770	51.1	38.6	10.3
0.8	-0.35937566	32.2	48.3	19.5	-0.38433191	36.1	46.9	17.0	-0.39617260	39.5	45.3	15.2
1.0	-0.36876131	7.9	51.4	40.7	-0.39005713	8.7	52.1	39.2	-0.39858414	9.7	52.8	37.5

	2^1A_1											
	cc-pVTZ-DK				cc-pVQZ-DK				cc-pV5Z-DK			
f	Energy	$d^{9\text{-}9}$	$d^{9\text{-}10}$	$d^{10\text{-}10}$	Energy	$d^{9\text{-}9}$	$d^{9\text{-}10}$	$d^{10\text{-}10}$	Energy	$d^{9\text{-}9}$	$d^{9\text{-}10}$	$d^{10\text{-}10}$
0.0	-0.30587555	46.4	41.8	11.8	-0.34090285	49.1	40.7	10.2	-0.35650604	51.2	39.8	9.0
0.2	-0.29956686	48.6	41.7	9.6	-0.33214487	52.5	39.8	7.7	-0.34702917	55.1	38.2	6.7
0.4	-0.28051688	48.2	41.4	10.3	-0.31046078	54.8	37.9	7.3	-0.32484879	58.9	35.6	5.5
0.6	-0.27090071	49.8	40.5	9.7	-0.30295571	84.0	15.1	1.0	-0.32076295	84.9	14.3	0.9
0.8	-0.27693258	25.7	59.0	15.3	-0.30059448	35.9	53.2	10.8	-0.31563413	85.0	14.3	0.8
1.0	-0.31486357	2.1	47.2	50.8	-0.33394938	2.6	51.8	45.5	-0.33980750	3.5	56.4	40.1

	3^1A_1											
	cc-pVTZ-DK				cc-pVQZ-DK				cc-pV5Z-DK			
f	Energy	$d^{9\text{-}9}$	$d^{9\text{-}10}$	$d^{10\text{-}10}$	Energy	$d^{9\text{-}9}$	$d^{9\text{-}10}$	$d^{10\text{-}10}$	Energy	$d^{9\text{-}9}$	$d^{9\text{-}10}$	$d^{10\text{-}10}$
0.0	-0.27269916	55.3	36.6	8.1	-0.30910599	60.5	33.7	5.8	-0.32545525	63.8	32.3	4.0
0.2	-0.27704793	55.6	36.6	7.8	-0.31087747	60.5	34.0	5.5	-0.32663255	63.8	31.9	4.2
0.4	-0.27119774	51.9	38.5	9.6	-0.30191815	58.4	35.3	6.3	-0.31678769	62.0	33.1	4.9
0.6	-0.26871440	82.6	16.2	1.2	-0.29951185	60.5	32.8	6.8	-0.31375753	68.6	27.0	4.4
0.8	-0.26513585	83.2	15.8	1.1	-0.29813597	83.8	15.2	1.0	-0.31129125	45.8	46.3	7.8
1.0	-0.27309887	2.9	95.8	1.3	-0.29491533	3.3	94.5	2.1	-0.30286683	4.1	92.9	3.0

	4^1A_1											
	cc-pVTZ-DK				cc-pVQZ-DK				cc-pV5Z-DK			
f	Energy	$d^{9\text{-}9}$	$d^{9\text{-}10}$	$d^{10\text{-}10}$	Energy	$d^{9\text{-}9}$	$d^{9\text{-}10}$	$d^{10\text{-}10}$	Energy	$d^{9\text{-}9}$	$d^{9\text{-}10}$	$d^{10\text{-}10}$
0.0	-0.26688457	58.9	34.5	6.6	-0.30361203	64.0	31.8	4.2	-0.32031090	66.5	30.4	3.1
0.2	-0.26739834	60.2	34.3	5.5	-0.30166345	64.2	31.7	4.0	-0.31784185	66.6	30.0	3.4
0.4	-0.25756449	71.1	25.4	3.5	-0.29239996	80.9	17.2	1.9	-0.31022812	83.1	15.3	1.5
0.6	-0.26057525	72.5	25.9	1.7	-0.29252571	75.2	23.7	1.1	-0.30824559	74.7	24.2	1.1
0.8	-0.25612262	74.1	23.7	2.2	-0.28729871	77.7	20.8	1.5	-0.30311413	78.8	20.1	1.1
1.0	-0.24541142	3.9	54.3	41.7	-0.26523602	70.5	27.5	2.0	-0.27874421	74.8	25.1	0.2

	5^1A_1											
	cc-pVTZ-DK				cc-pVQZ-DK				cc-pV5Z-DK			
f	Energy	$d^{9\text{-}9}$	$d^{9\text{-}10}$	$d^{10\text{-}10}$	Energy	$d^{9\text{-}9}$	$d^{9\text{-}10}$	$d^{10\text{-}10}$	Energy	$d^{9\text{-}9}$	$d^{9\text{-}10}$	$d^{10\text{-}10}$
0.0	-0.2554919	62.6	31.3	6.1	-0.29252359	65.4	29.6	5.1	-0.30909802	67.4	28.3	4.3
0.2	-0.2549316	59.5	33.8	6.7	-0.28901029	62.8	31.7	5.4	-0.30482757	65.1	30.2	4.7
0.4	-0.2553921	76.7	21.1	2.2	-0.28973251	73.9	23.8	2.3	-0.30613679	75.4	22.6	2.0
0.6	-0.2519646	88.3	11.2	0.6	-0.28595159	90.2	9.5	0.3	-0.30355596	91.0	9.0	0.0
0.8	-0.2469300	89.8	9.9	0.4	-0.27972290	90.5	9.2	0.3	-0.29688694	91.0	8.7	0.2
1.0	-0.2388225	72.0	27.7	0.3	-0.26400838	7.8	48.7	43.5	-0.26883420	8.4	44.6	47.0

Table S5 RAS(28,18)PFRS-V1 five low-lying states dependence with the basis set. Total energies+3455 in atomic unities (E_h) and the d columns represent the sum of squared coefficient (in percentage) for each pair of d-occupancies in each root wave function

	1^1A_1						
f	RAS(4,4)	NEVPT2	CASPT2	REPT2	$d^{9\text{-}9}$	$d^{9\text{-}10}$	$d^{10\text{-}10}$
0.0	-5.076008931849	-6.482742074632	-6.592454083774	-6.553027152147	54	40	7
0.2	-5.105069257572	-6.490003189483	-6.579845738812	-6.538317910936	53	40	7
0.4	-5.131270150456	-6.498073540514	-6.578630729245	-6.524730100568	52	40	8
0.6	-5.157839510466	-6.509644962448	-6.572479229768	-6.518877164736	49	42	9
0.8	-5.181876134111	-6.520944878557	-6.565712811572	-6.521286341662	41	47	13
1.0	-5.195973381544	-6.525111482554	-6.553912902983	-6.522719522944	25	56	20

	2^1A_1						
f	RAS(4,4)	NEVPT2	CASPT2	REPT2	$d^{9\text{-}9}$	$d^{9\text{-}10}$	$d^{10\text{-}10}$
0.0	-4.961785875816	-6.369961590770	-6.564065239768	-6.409699673308	86	14	0
0.2	-5.003994927622	-6.385909435797	-6.513375496142	-6.420384685876	82	18	0
0.4	-5.031955330786	-6.393880698707	-6.512673818056	-6.401675295070	77	23	0
0.6	-5.037149238184	-6.383745486080	-6.459608469509	-6.479837154850	70	29	1
0.8	-5.016990679441	-6.389023466736	-6.461932722828	-6.427568304505	64	27	9
1.0	-5.046442334119	-6.407884623148	-6.458058099990	-6.432178233739	0	100	0

	3^1A_1						
f	RAS(4,4)	NEVPT2	CASPT2	REPT2	$d^{9\text{-}9}$	$d^{9\text{-}10}$	$d^{10\text{-}10}$
0.0	-4.918387163527	-6.333680304358	-6.595844135517	-6.354333492794	79	21	0
0.2	-4.940469358405	-6.334564161370	-6.387806938738	-6.243113662153	77	23	0
0.4	-4.952713565868	-6.330651265209	-6.460829250270	-6.440842977748	73	27	0
0.6	-4.953796543367	-6.346725835346	-6.416574846926	-6.433225142223	53	47	0
0.8	-4.992666445568	-6.364231297328	-6.425094545170	-6.426330254941	2	98	0
1.0	-5.015570784934	-6.380719869863	-6.430441278434	-6.416346559162	69	07	23

	4^1A_1						
f	RAS(4,4)	NEVPT2	CASPT2	REPT2	$d^{9\text{-}9}$	$d^{9\text{-}10}$	$d^{10\text{-}10}$
0.0	-4.790594541002	-6.242873096019	-6.290353760710	-6.112236908397	83	17	0
0.2	-4.791046791365	-6.251128040359	-6.919185548417	-6.534260946830	60	32	7
0.4	-4.847755974534	-6.307654256614	-6.478183147804	-6.403245913913	5	95	0
0.6	-4.910880789774	-6.318711038677	-6.460731678139	-6.397394917952	43	32	25
0.8	-4.955180534927	-6.247555218115	-6.317577851380	-6.282370560751	50	33	17
1.0	-4.893239947785	-6.152916384746	-6.227513500632	-6.177144261676	47	51	2

	1^5A_1						
f	RAS(4,4)	NEVPT2	CASPT2	REPT2	$d^{9\text{-}9}$	$d^{9\text{-}10}$	$d^{10\text{-}10}$
0.0	-4.729756737901	-6.254737484541	-6.378017824205	-6.427810853429	3	97	0
0.2	-4.785743575477	-6.279838655338	-6.430609647956	-6.408240883807	3	97	0
0.4	-4.846786892255	-6.318813302286	-6.369814375594	-6.443104332503	37	38	25
0.6	-4.909570255502	-6.335051238006	-6.423691327031	-6.407777599091	19	81	0
0.8	-4.904338816918	-6.343544656931	-6.445168267336	-6.433716237661	58	42	0
1.0	-4.820259375302	-6.224572279912	-6.275831472721	-6.231267597508	38	62	0

Table S6 Bare $[Cu_2O_2]^{2+}$ core total energies+3450 E_h for the five low-lying A_1 states obtained using RAS(4,4)PFRS-V1 (cc-pVDZ-DK basis set) and perturbative corrections over the CAS(4,4)CI reference wave function using the RAS orbitals. Columns labeled as d represents the sum of squared coefficient (in percentage) for each pair of d-occupancies in each root wave function.

	1^1A_1				
f	MRCISD	MRCISD+Q	$d^{9\text{-}9}$	$d^{9\text{-}10}$	$d^{10\text{-}10}$
0.0	-6.086914446894	-6.28920516	40	36	8
0.2	-6.108648292477	-6.30451791	49	36	8
0.4	-6.128842587139	-6.31870768	37	37	10
0.6	-6.150737461419	-6.33465885	29	39	12
0.8	-6.171863581539	-6.34987535	26	43	16
1.0	-6.185539044417	-6.35785065	14	47	25

	2^1A_1				
f	MRCISD	MRCISD+Q	$d^{9\text{-}9}$	$d^{9\text{-}10}$	$d^{10\text{-}10}$
0.0	-5.968209120572	-6.17591405	68	15	0
0.2	-6.001087285411	-6.19947343	65	18	0
0.4	-6.021414534743	-6.21166678	62	22	0
0.6	-6.020885274336	-6.20471109	57	25	2
0.8	-6.006284377107	-6.19804697	01	83	1
1.0	-6.045471345198	-6.22452640	00	85	0

	3^1A_1				
f	MRCISD	MRCISD+Q	$d^{9\text{-}9}$	$d^{9\text{-}10}$	$d^{10\text{-}10}$
0.0	-5.927700881603	-6.13692269	60	23	0
0.2	-5.942523282141	-6.14476490	58	25	0
0.4	-5.950200206703	-6.14742202	51	33	0
0.6	-5.962511811413	-6.16300949	25	68	0
0.8	-6.006978775236	-6.19400094	56	14	15
1.0	-6.011457888366	-6.19825935	60	1	23

	4^1A_1				
f	MRCISD	MRCISD+Q	$d^{9\text{-}9}$	$d^{9\text{-}10}$	$d^{10\text{-}10}$
0.0	-5.791398057280	-6.02847974	5	77	0
0.2	-5.834876371519	-6.06584731	6	76	1
0.4	-5.887238907160	-6.10705918	11	72	0
0.6	-5.936357237545	-6.14329306	41	20	22
0.8	-5.953912734831	-6.14028426	44	31	9
1.0	-5.848917090902	-6.05276704	28	57	0

	5^1A_1				
f	MRCISD	MRCISD+Q	$d^{9\text{-}9}$	$d^{9\text{-}10}$	$d^{10\text{-}10}$
0.0	-5.779970812017	-6.02476208	36	19	27
0.2	-5.836090226239	-6.06253055	33	26	23
0.4	-5.883875092864	-6.09660629	36	23	24
0.6	-5.915461354459	-6.10573238	41	43	0
0.8	-5.886901270748	-6.06721513	45	40	0
1.0	-5.869949435432	-6.04458563	38	46	1

Table S7 Bare $[Cu_2O_2]^{2+}$ core total energies+3450 E_h for the five low-lying A_1 states obtained using CAS(4,4)CI/MRCISD and with the Davidson correction (+Q), based on the RAS(4,4)PFRS-V1 orbitals(cc-pVDZ-DK basis set) . Columns labeled as d represents the sum of squared coefficient (in percentage) for each pair of d-occupancies in each root reference wave function at the final MRCISD wave function normalization.

f	MRCCSD	MRCCSD(T)	$d^{9\text{-}9}$	$d^{9\text{-}10}$	$d^{10\text{-}10}$
0.0	-6.336808229600	-6.351230537355	45	43	10
0.4	-6.367077472143	-6.377881505513	42	45	13
0.6	-6.379923357877	-6.390988798942	37	47	16
0.8	-6.389298541626	-6.402087124357	28	51	21
1.0	-6.391049487163	-6.404417084605	14	53	33

Table S8 Bare $[Cu_2O_2]^{2+}$ core total energies+3450 E_h for the lowest energy A_1 state obtained using CAS(4,4)CI/MRCCSD and CAS(4,4)CI/MRCCSD(T) methods, based on the RAS(4,4)PFRS-V1 orbitals(cc-pVDZ-DK basis set) . Columns labeled as d represents the sum of squared coefficient (in percentage) for each pair of d-occupancies in the relaxed reference wave function at the final MRCCSD intermediate normalization.

	RAS(4,4)PFRS-V1											
	cc-pVTZ-DK				cc-pVQZ-DK				cc-pV5Z-DK			
f	Energy	$d^{9\text{-}9}$	$d^{9\text{-}10}$	$d^{10\text{-}10}$	Energy	$d^{9\text{-}9}$	$d^{9\text{-}10}$	$d^{10\text{-}10}$	Energy	$d^{9\text{-}9}$	$d^{9\text{-}10}$	$d^{10\text{-}10}$
0.0	-5.1403817	56	38	6	-5.1777742	57	37	6	-5.1940035	58	36	6
0.2	-5.1652489	55	38	7	-5.1996713	57	37	6	-5.2154818	58	36	6
0.4	-5.1882571	55	38	7	-5.2201994	56	37	7	-5.2356783	58	36	6
0.6	-5.2124288	52	40	8	-5.2421491	54	38	8	-5.2356783	58	36	6
0.8	-5.2349865	44	45	11	-5.2622492	47	43	10	-5.2755856	49	42	9
1.0	-5.2482651	28	54	18	-5.2729908	30	53	17	-5.2844101	32	52	16

	MRCISD											
	cc-pVTZ-DK				cc-pVQZ-DK				cc-pV5Z-DK			
f	Energy	$d^{9\text{-}9}$	$d^{9\text{-}10}$	$d^{10\text{-}10}$	Energy	$d^{9\text{-}9}$	$d^{9\text{-}10}$	$d^{10\text{-}10}$	Energy	$d^{9\text{-}9}$	$d^{9\text{-}10}$	$d^{10\text{-}10}$
0.0	-6.311167	43	33	7	-6.4161929	44	35	7	-6.4591249	44	34	6
0.2	-6.331763	42	35	7	-6.4354774	43	35	7	-6.4780585	43	35	7
0.4	-6.351332	40	35	9	-6.4537554	42	35	8	-6.4960246	42	35	8
0.6	-6.372948	37	38	10	-6.4741973	38	37	10	-6.5160138	39	37	10
0.8	-6.394193	30	42	14	-6.4942355	31	41	13	-6.5354229	32	41	13
1.0	-6.407884	16	47	23	-6.5071009	18	46	22	-6.5475864	18	46	21

	MRCISD+Q		
	cc-pVTZ-DK	cc-pVQZ-DK	cc-pV5Z-DK
f	Energy	Energy	Energy
0.0	-6.53044551	-6.64067166	-6.68383082
0.2	-6.54674204	-6.65688389	-6.69984246
0.4	-6.56221253	-6.67207714	-6.71485847
0.6	-6.57970891	-6.68936118	-6.73200409
0.8	-6.59675282	-6.70625750	-6.74882306
1.0	-6.60599836	-6.71580808	-6.75828549

	MRCCSD											
	cc-pVTZ-DK				cc-pVQZ-DK				cc-pV5Z-DK			
f	Energy	$d^{9\text{-}9}$	$d^{9\text{-}10}$	$d^{10\text{-}10}$	Energy	$d^{9\text{-}9}$	$d^{9\text{-}10}$	$d^{10\text{-}10}$	Energy	$d^{9\text{-}9}$	$d^{9\text{-}10}$	$d^{10\text{-}10}$
0.0	-6.58754895	46	43	10	-6.70151766	46	42	10				
0.2	-6.60547424	45	43	11	-6.71877438	45	43	11				
0.4	-6.61788656	43	44	13	-6.73106007	43	44	12				
0.6	-6.63174650	38	47	15	-6.74490350	39	46	15				
0.8	-6.64264350	29	51	21	-6.75588072	30	50	20				
1.0	-6.64537412	15	52	33	-6.75902724	15	52	32				

	MRCCSD(T)		
	cc-pVTZ-DK	cc-pVQZ-DK	cc-pV5Z-DK
f	Energy	Energy	Energy
0.0	-6.61111154	-6.72858368	
0.2	-6.62279651	-6.73956590	
0.4	-6.63748193	-6.75406644	
0.6	-6.65156699	-6.76808490	
0.8	-6.66457341	-6.78156163	
1.0	-6.66794635	-6.78568335	

Table S9 Tables S6, S7 and S8 results dependence with the basis set size.

	b_{3u}			b_{2g}			Wave Function		
f	occ.	$3d_{xz}$	$2p_x$	occ.	$3d_{xz}$	$2p_z$	$\|b_{3u}^2\rangle$	$\|b_{2g}^2\rangle$	Total Energy
0.0	1.26	1.00	0.11	0.73	0.959	0.376	0.79481527	-0.60685146	-3455.06152580
0.2	1.29	1.00	0.17	0.71	0.955	0.392	0.80208008	-0.59721650	-3455.10793786
0.4	1.31	1.00	0.16	0.68	0.946	0.413	0.81169877	-0.58407629	-3455.14809556
0.6	1.37	1.00	0.15	0.63	0.928	0.445	0.82716087	-0.56196521	-3455.18119767
0.8	1.47	1.00	0.12	0.53	0.888	0.501	0.85692039	-0.51544879	-3455.20431040
1.0	1.69	1.00	0.06	0.31	0.787	0.600	0.91942150	-0.39327358	-3455.21445310

Table S10 Active orbitals and wave function composition for the bare $[Cu_2O_2]^{2+}$ core ground state at the PFRS-V2/CAS(2,2)/cc-pVDZ-DK level of theory.

	CAS(2,2)PFRS-V2			
f	cc-pVDZ-DK	cc-pVTZ-DK	cc-pVQZ-DK	cc-pV5Z-DK
0.0	-3455.061525799425	-3455.138049214575	-3455.186551076481	-3455.215401644103
0.2	-3455.107937863600	-3455.178216417526	-3455.222565831683	-3455.251016375517
0.4	-3455.148095555251	-3455.213750615887	-3455.254915316254	-3455.283154537965
0.6	-3455.181197674141	-3455.243577725330	-3455.281837949717	-3455.309341308860
0.8	-3455.204310403086	-3455.264238762494	-3455.298813548553	-3455.324468094329
1.0	-3455.214453102953	-3455.270721134635	-3455.298713659799	-3455.319256974977

	MRCISD			
f	cc-pVDZ-DK	cc-pVTZ-DK	cc-pVQZ-DK	cc-pV5Z-DK
0.2	-3456.080817224151	-3456.307733086640	-3456.414755818100	-3456.461459812631
0.4	-3456.115269580867	-3456.341213319287	-3456.446417511756	-3456.492576942270
0.6	-3456.144906797097	-3456.370122266963	-3456.473435336210	-3456.518671928954
0.8	-3456.167940644543	-3456.392326019983	-3456.492876001920	-3456.536101991030
1.0	-3456.184009539263	-3456.407176845225	-3456.503717284370	-3456.541002202881

	MRCISD+Q			
f	cc-pVDZ-DK	cc-pVTZ-DK	cc-pVQZ-DK	cc-pV5Z-DK
0.0	-3456.23171655	-3456.47165056	-3456.58313136	-3456.62799205
0.2	-3456.26292504	-3456.50436553	-3456.61545353	-3456.65982466
0.4	-3456.29055153	-3456.53366373	-3456.64404106	-3456.68790840
0.6	-3456.31402032	-3456.55859446	-3456.66800186	-3456.71105576
0.8	-3456.33173880	-3456.57738905	-3456.68501923	-3456.72626358
1.0	-3456.34285929	-3456.58977410	-3456.69558441	-3456.73159768

	MRCCSD			
f	cc-pVDZ-DK	cc-pVTZ-DK	cc-pVQZ-DK	cc-pV5Z-DK
0.0	-3456.310052313908	-3456.558972437527	-3456.673385908913	
0.2	-3456.330364135201	-3456.579177230692	-3456.693165443877	
0.4	-3456.349235376012	-3456.598895408300	-3456.712571683085	
0.6	-3456.366350744167	-3456.617453448146	-3456.730967797455	
0.8	-3456.379585437262	-3456.632444288427	-3456.745787276236	
1.0	-3456.385086222011	-3456.639179056043	-3456.752845174834	

	MRCCSD(T)			
f	cc-pVDZ-DK	cc-pVTZ-DK	cc-pVQZ-DK	cc-pV5Z-DK
0.0	-3456.341051679557	-3456.576421864439		
0.2	-3456.350511093044	-3456.591620648298		
0.4	-3456.362552594779	-3456.607801144855		
0.6	-3456.376247874569	-3456.624679188141		
0.8	-3456.388271940901	-3456.639339550111		
1.0	-3456.393546375196	-3456.646511504697		

Table S11 Bare $[Cu_2O_2]^{2+}$ core total energies in E_h for the A_1 lowest state obtained using CAS(2,2)PFRS-V2 and post-CASCI methods and their dependence with the basis set.

	CAS(12,8)PFRS-V2			
f	cc-pVDZ-DK	cc-pVTZ-DK	cc-pVQZ-DK	cc-pV5Z-DK
0.0	-3455.200372518656	-3455.257930342166	-3455.291379586452	-3455.308675863316
0.2	-3455.217530536539	-3455.270516320786	-3455.300252839344	-3455.316455816277
0.4	-3455.232183098369	-3455.281218837346	-3455.306921060072	-3455.319187252091
0.6	-3455.247155101940	-3455.293825338159	-3455.316925829007	-3455.327414534136
0.8	-3455.265214953815	-3455.311452768700	-3455.332515693518	-3455.340649435073
1.0	-3455.270910556121	-3455.316982418502	-3455.336261383760	-3455.343464188798

	MRCISD			
f	cc-pVDZ-DK	cc-pVTZ-DK	cc-pVQZ-DK	cc-pV5Z-DK
0.0	-3456.151076872576	-3456.377545640220	-3456.482882591671	-3456.526794765548
0.2	-3456.168199400555	-3456.392529506437	-3456.495987034573	-3456.539326791564
0.4	-3456.182547967565	-3456.405215485197	-3456.506592480577	-3456.548076209526
0.6	-3456.196835093790	-3456.418854797620	-3456.518945900975	-3456.559689367004
0.8	-3456.212171965951	-3456.434812310286	-3456.533977673498	-3456.573892489855
1.0	-3456.219970328508	-3456.443039213008	-3456.541664666523	-3456.581142522903

	MRCISD+Q			
f	cc-pVDZ-DK	cc-pVTZ-DK	cc-pVQZ-DK	cc-pV5Z-DK
0.0	-3456.31212025	-3456.55896834	-3456.67188048	-3456.71618271
0.2	-3456.32822446	-3456.57475223	-3456.68689933	-3456.73081122
0.4	-3456.34106619	-3456.58780968	-3456.69913859	-3456.74227743
0.6	-3456.35298253	-3456.60065256	-3456.71158603	-3456.75450850
0.8	-3456.36399842	-3456.61347104	-3456.72425611	-3456.76719068
1.0	-3456.36844028	-3456.61914806	-3456.73023399	-3456.77309576

Table S12 Bare $[Cu_2O_2]^{2+}$ core total energies in E_h for the A_1 lowest state obtained using CAS(12,8)PFRS-V2 and post-CASCI methods and their dependence with the basis set.

	CAS(2,2)PFRS-V2/NEVPT2			
f	cc-pVDZ-DK†	cc-pVTZ-DK†	cc-pVQZ-DK†	cc-pV5Z-DK†
0.0	-3456.399356334397	-3456.654993637240	-3456.765903693881	-3456.802744768832
0.2	-3456.423964578384	-3456.684536752476	-3456.796537874839	-3456.832461641252
0.4	-3456.446973759746	-3456.711088154985	-3456.823003127695	-3456.857831229616
0.6	-3456.467625787425	-3456.733834466062	-3456.845246678864	-3456.878609034714
0.8	-3456.484219770065	-3456.751805947358	-3456.862138742605	-3456.893069930778
1.0	-3456.496338462362	-3456.767568752436	-3456.879053846977	-3456.903722623148

	CAS(4,4)PFRS-V1/NEVPT2			
f	cc-pVDZ-DK*	cc-pVTZ-DK*	cc-pVQZ-DK*	cc-pV5Z-DK†
0.0	-3456.482742074632	-3456.766669208898	-3456.88416673841584	-3456.934670237722
0.2	-3456.490003189483	-3456.775525606069	-3456.89257044791384	-3456.942948560301
0.4	-3456.498073540514	-3456.785277393459	-3456.90116725332064	-3456.951348462001
0.6	-3456.509644962448	-3456.798636929803	-3456.91337485700660	-3456.963513176791
0.8	-3456.520944878557	-3456.811810050246	-3456.92596541154580	-3456.976464161634
1.0	-3456.525111482554	-3456.816313243738	-3456.93247211457901	-3456.984588494769

	CAS(12,8)PFRS-V2/NEVPT2			
f	cc-pVDZ-DK†	cc-pVTZ-DK†	cc-pVQZ-DK†	cc-pV5Z-DK†
0.0	-3456.468133062860	-3456.742034728502	-3456.870726278591	-3456.921167799275
0.2	-3456.486082473820	-3456.760700068134	-3456.890334065353	-3456.941750698519
0.4	-3456.499520842217	-3456.774986372933	-3456.905312129779	-3456.958811596726
0.6	-3456.511530563591	-3456.787881163519	-3456.918294188480	-3456.972523019797
0.8	-3456.520091548104	-3456.797497589463	-3456.927476760882	-3456.982448091086
1.0	-3456.524914841607	-3456.804111188343	-3456.934364959869	-3456.988883406701

Table S13 Bare $[Cu_2O_2]^{2+}$ core ground state total energies (in E_h) for a set of basis sets and active spaces. * Results using GeCCo implementation; and † using MOLPRO partially contracted implementation.

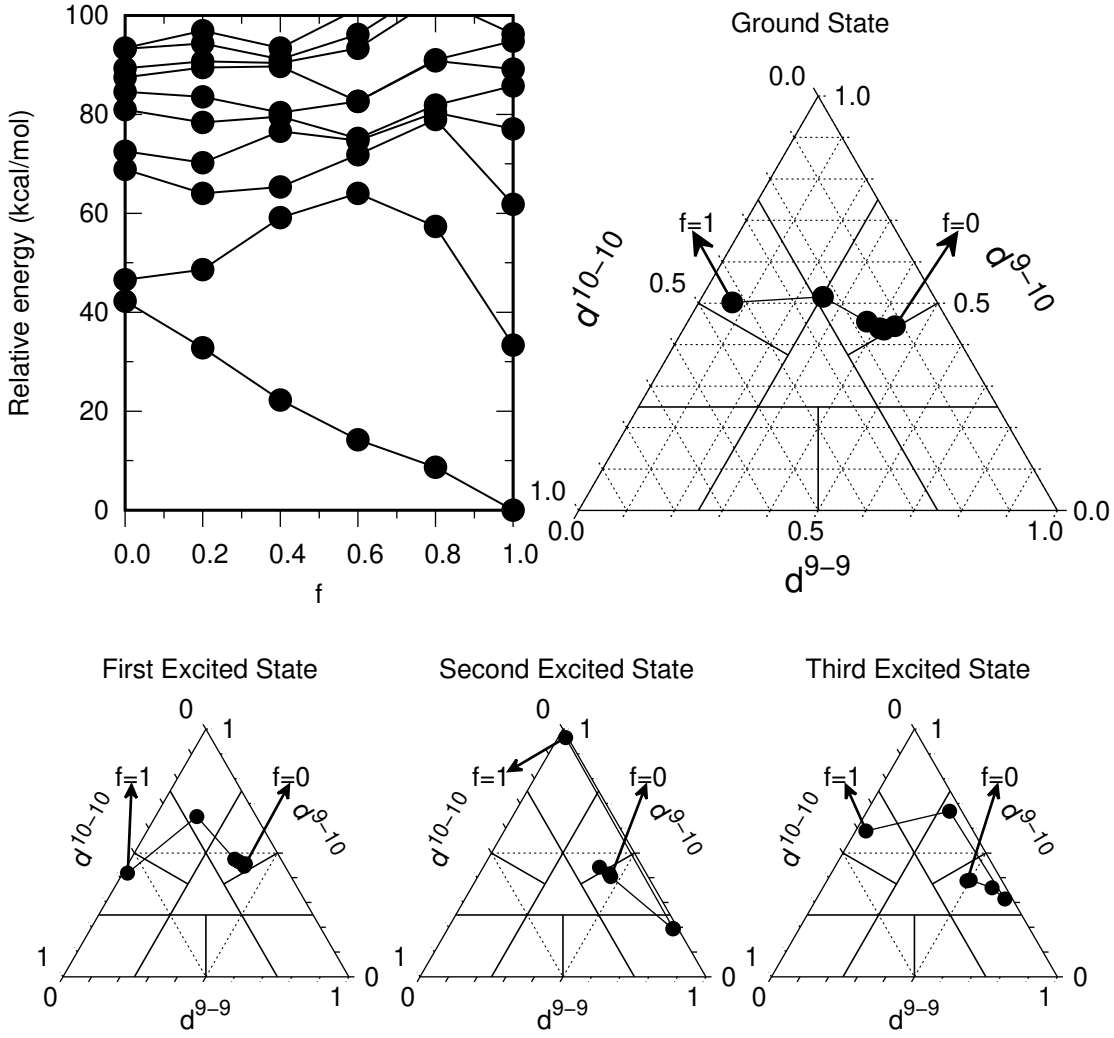

Fig. S2 Monochromatic version of Figure 5 of the main text. Each ternary diagram represents the d-pair occupancy weight vector for the state specified in the label above it. The geometry extremes are marked in each case with "f=0" and "f=1". The numerical data can be found in Tables S4

Notes and references

1 P. J. Hay, *J. Chem. Phys.*, 1977, 66, 4377–4384.
2 M. M. F. de Moraes, *Ph.D. thesis*, Federal University of ABC, Santo André-SP, Brazil, 2023.
3 M. M. F. de Moraes and Y. A. Aoto, *J. Phys. Chem. A*, 2023, 127, 10075.
4 M. M. F. de Moraes and Y. A. Aoto, *Theor. Chem. Acc.*, 2020, 139, 71.
5 B. F. Gherman and C. J. Cramer, *Coord. Chem. Rev.*, 2009, 253, 723–753.
6 M. Hanauer, *Ph.D. thesis*, Johannes Gutenberg-Universität, Mainz, 2013.
7 M. Hanauer and A. Köhn, *J. Chem. Phys.*, 2011, 134, 204111.
8 C. J. Cramer, M. Włoch, P. Piecuch, C. Puzzarini and L. Gagliardi, *J. Phys. Chem. A*, 2006, 110, 1991–2004.
9 Y. Kurashige and T. Yanai, *J. Chem. Phys.*, 2009, 130, 234114.

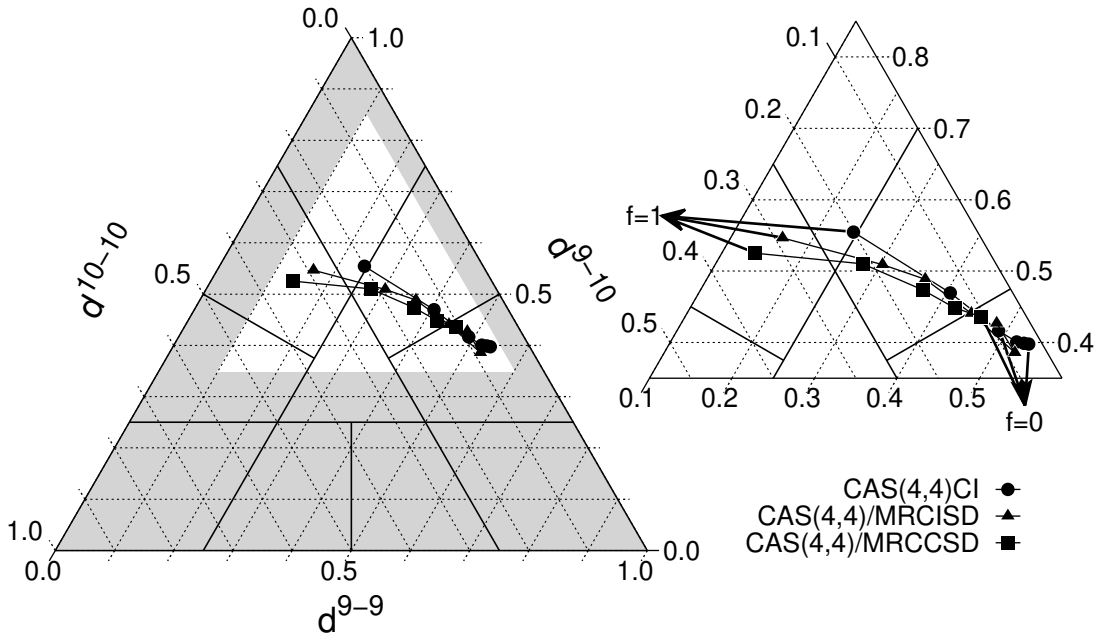

Fig. S3 Monochromatic ternary diagram for the d-pair occupancy weight of Figure 6 ground states. The right inset graph is an amplified version of the white section of the main graph (at left). The geometry extremes are marked with "f=0" and "f=1". The numerical data can be found in Tables S6-S8.

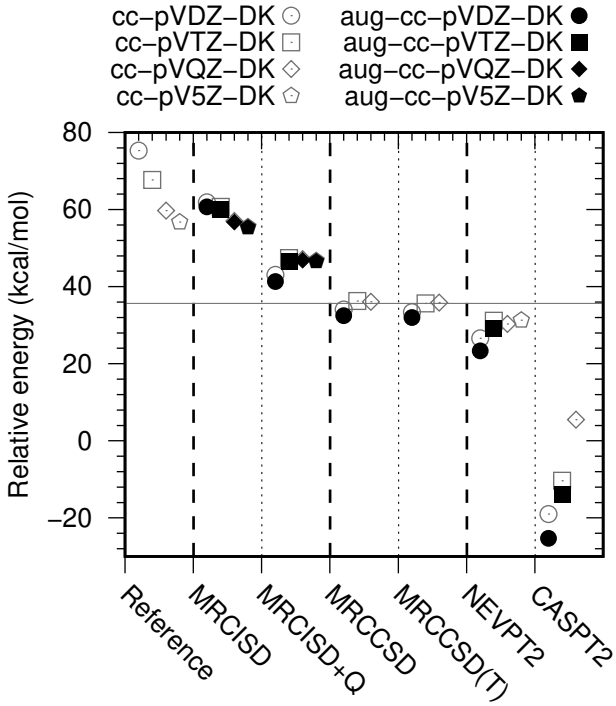

Fig. S4 Comparison between the post-CAS(4,4)CI results shown in Figure 7 of the main text (hollow grey points) with the addition of augmented basis sets (black filled points). The gray line marks the DMRG(32,62) relative energy—states with d^8-occupancies for the $[Cu_2O_2]^{2+}$ model system.[9]

	2O/2P						
	Occupation-Specific			RAS(28,18)PFRS-V1			
f	E$d^{9\text{-}9}$	E$d^{9\text{-}10}$	E$d^{10\text{-}10}$	Energy	$d^{9\text{-}9}$	$d^{9\text{-}10}$	$d^{10\text{-}10}$
0.0	-0.403018251408	-0.267860287966	-0.026782692783	-0.472484035919	60	35	5
0.2	-0.435014587944	-0.299218131122	-0.055942248726	-0.492909948527	64	32	5
0.4	-0.462460036683	-0.281087124634	-0.094742934219	-0.513341215255	65	31	5
0.6	-0.483150121420	-0.330815912100	-0.144104614393	-0.533009062548	62	33	6
0.8	-0.492168167653	-0.379972305718	-0.205735827114	-0.534042362243	59	35	6
1.0	-0.472993295412	-0.412666406461	-0.270988896903	-0.514773129479	52	39	8

	3O/3P						
	Occupation-Specific			RAS(28,18)PFRS-V1			
f	E$d^{9\text{-}9}$	E$d^{9\text{-}10}$	E$d^{10\text{-}10}$	Energy	$d^{9\text{-}9}$	$d^{9\text{-}10}$	$d^{10\text{-}10}$
0.0	-3680.411493447462	-0.269179977269 (-0.265216304566)	-0.042276093643	-0.441426773059	69	29	2
0.2	-3680.440149542063	-0.297402528000 (-0.292201129024)	-0.067545969433	-0.458918222369	70	27	3
0.4	-3680.465656880718	-0.277992116564 (-0.271129768568)	-0.103201557799	-0.478270155537	70	27	3
0.6	-3680.484787627318	-0.325494786724 (-0.318664978410)	-0.150104051498	-0.496267595279	65	30	5
0.8	-3680.492859035226	-0.365063413640 (-0.372798624941)	-0.209845740611	-0.496745521056	63	32	5
1.0	-3680.475280043215	-0.396230563869 (-0.402102054748)	-0.273777378008	-0.476951750534	56	37	7

	4O/4P						
	Occupation-Specific			RAS(28,18)PFRS-V1			
f	E$d^{9\text{-}9}$	E$d^{9\text{-}10}$	E$d^{10\text{-}10}$	Energy	$d^{9\text{-}9}$	$d^{9\text{-}10}$	$d^{10\text{-}10}$
0.0	-0.419065264061	-0.293209830238	-0.058210531610	-0.412461393431	70	26	2
0.2	-0.445096098766	-0.316877740434	-0.079727158006	-0.432772190098	81	19	1
0.4	-0.468939793868	-0.348891624690	-0.112214909405	-0.452742587004	81	18	1
0.6	-0.486639451728	-0.330054008200	-0.156535800867	-0.465401035308	82	17	1
0.8	-0.493346416504	-0.367433014391	-0.214241192892	-0.465537291100	83	17	1
1.0	-0.475118158356	-0.398001315024	-0.276700433305	-0.437368615461	81	18	1

Table S14 Total energy +3680 (E_h) for the lowest energy states of Figure 8. d-occupancy specific represented by "Ed" columns, "Energy" column represents the results using an intermediary size of d-orbitals, "d" columns represents the sum of squared coefficient (in percentage) for the given pair of d-occupancies.

	svd threshold			
f	10^{-4}	10^{-5}	10^{-6}	10^{-7}
0.000	-3682.541585161860	-3682.547234938139	—	—
0.050		-3682.549040114318		
0.100	-3682.543178090925	-3682.549864138478	-3682.549456181528	
0.125		-3682.550262577298		
0.150		-3682.550777710173		
0.175		—		
0.200	-3682.543553295366	—	-3682.54996876 (-7)	
0.225		-3682.547777997587		
0.250		-3682.547660550980		
0.275		-3682.547515669245		
0.300	-3682.543126065674	-3682.547129825804	-3682.546515865497	—
0.350		-3682.546590849289	—	
0.400	-3682.543279157594	-3682.546760235530	-3682.54647707 (-5)	-3682.546477248467
0.450		-3682.54819220 (-5)	-3682.548437647517	
0.500	-3682.545022844603	-3682.548622601998	-3682.54875723 (-6)	
0.550		-3682.549807733527		
0.600	-3682.548399822256	-3682.551410595878	-3682.55152403 (-5)	
0.650		-3682.552584626827		
0.700	-3682.553044660732	—	—	—
0.750		-3682.554532409757		
0.800	-3682.553717363200	-3682.554911213206	-3682.554879028856	-3682.556400124879
0.850		-3682.554307853525		
0.900	-3682.551746136159	-3682.55272093 (-7)	-3682.552713605707	
0.950		-3682.550129726169		
1.000	-3682.545365223263	-3682.545768275509	-3682.546211095851	-3682.547274934107

Table S15 CAS(4,4)PFRS-V2/MRCCSD total energies (E_h) for the 2O/2P equilibrium. Column numbers represents the svd threshold value used. Blank entries indicates that the calculation was not attempted. '—' indicates that after at least 200 iteration the residual has shown no trend towards convergence. Values with parenthesis indicate that the residual showed a convergence trend, but didn't reached the default threshold of 10^{-8} before the reach the calculation memory or time limits. The values within the parenthesis are the residual order of magnitude at the last iteration.

	Active Space			
f	(4,4)	(12,8)	(16,10)	(12,10)
0.000	-0.561140389301	-0.510579122120	-0.472086053119	-0.529885201579
0.025	-0.560898587747	-0.511263585272	-0.473472275784	-0.530464641264
0.050	-0.560515726478	-0.511818385405	-0.474753771670	-0.530921854888
0.075	-0.559997200808	-0.512252325368	-0.475927981894	-0.531263849041
0.100	-0.559348164923	-0.512576730498	-0.476991425006	-0.531498407551
0.125	-0.558573464384	-0.512806035103	-0.477940773303	-0.531634532445
0.150	-0.557677520093	-0.512958111585	-0.478773620198	-0.531682644187
0.175	-0.556664087762	-0.513054301246	-0.479489510732	-0.531654979798
0.200	-0.555536482978	-0.513118817664	-0.480090954170	-0.531565865161
0.225	-0.554297045958	-0.513177936729	-0.480588644937	-0.531432009141
0.250	-0.552948271407	-0.513258631769	-0.480998315741	-0.531272396977
0.275	-0.551493029489	-0.513387173581	-0.481346052718	-0.531108563406
0.300	-0.549936359298	-0.513587728399	-0.481660709765	-0.530963052559
0.325	-0.548289336964	-0.513881117113	-0.481973510947	-0.530859330505
0.350	-0.546571752251	-0.514284044355	-0.482316015546	-0.530819998239
0.375	-0.544819998435	-0.514808656185	-0.482712650169	-0.530865318121
0.400	-0.543088805704	-0.515462645369	-0.483185763855	-0.531012113486
0.425	-0.541448804660	-0.516249837601	-0.483755815411	-0.531272234143
0.450	-0.539977454034	-0.517172262849	-0.484439053833	-0.531651561263
0.475	-0.538743076602	-0.518229438644	-0.485253104678	-0.532150161639
0.500	-0.537788683211	-0.519418209266	-0.486211535199	-0.532762524694
0.525	-0.537132243096	-0.520730328101	-0.487333524353	-0.533477365575
0.550	-0.536760438434	-0.522151621105	-0.488617334183	-0.534278984752
0.575	-0.536637923220	-0.523662560932	-0.490080332175	-0.535148212190
0.600	-0.536713517827	-0.525239918403	-0.491699454060	-0.536062985058
0.625	-0.536924649492	-0.526858284001	-0.493457134522	-0.536999467196
0.650	-0.537210794549	-0.528491483511	-0.495364851507	-0.537932728226
0.675	-0.537508835932	-0.530112797333	-0.497401061437	-0.538836982827
0.700	-0.537761034850	-0.531695728305	-0.499580569177	-0.539687275673
0.725	-0.537911654308	-0.533214013093	-0.501878154726	-0.540458526803
0.750	-0.537913066368	-0.534641602425	-0.504296589334	-0.541126431875
0.775	-0.537724123071	-0.535952571049	-0.506786732893	-0.541668124620
0.800	-0.537310598542	-0.537121714609	-0.509287576995	-0.542062049395
0.825	-0.536646047354	-0.538124378993	-0.511691203677	-0.542288462667
0.850	-0.535712396338	-0.538936992469	-0.513898949439	-0.542329614007
0.875	-0.534500387563	-0.539536938805	-0.515842438864	-0.542170151208
0.900	-0.533009682446	-0.539904141036	-0.517476282156	-0.541797502101
0.925	-0.531248459401	-0.540020880535	-0.518784972625	-0.541202211031
0.950	-0.529232423211	-0.539873970210	-0.519770059299	-0.540378861872
0.975	-0.526983361483	-0.539457086034	-0.520446312182	-0.539326693116
1.000	-0.524527848156	-0.538775128031	-0.520836350278	-0.538050917524

Table S16 CAS(X,Y)PFRS-V2/NEVPT2 total energy plus 3682 E_h for the 2O/2P equilibrium. Each column indicates the active space given by "(X,Y)".